

Bragg Diffraction in Atomic Systems in Quantum Degeneracy Conditions

V. M. Porozova^a, V. A. Pivovarov^a, L. V. Gerasimov^{a, b}, and D. V. Kupriyanov^{a, *}

^a *Laboratory of Quantum Optics and Quantum Informatics, Center for Advanced Studies,
Peter the Great St. Petersburg Polytechnic University, St. Petersburg, 195251 Russia*

^b *Quantum Technology Center, Faculty of Physics, Moscow State University,
Moscow, 119991 Russia*

**e-mail: kupr@dk11578.spb.edu*

Received October 12, 2018

Studies of the scattering of light on systems of identical atoms under conditions of their quantum degeneracy have been reviewed. The formation of a periodic spatial structure caused by the interference of material waves is responsible for coherent resonance scattering similar to Bragg diffraction on regular spatial inhomogeneities. The interference of macroscopic material waves that is observed in experiments with a Bose–Einstein condensate forms a dielectric medium in the region of optical transparency of the sample that has the properties of a photonic crystal. Common characteristics and differences between the scattering of light on atomic systems under quantum degeneracy conditions and scattering on one-dimensional atomic lattices where the positions of atoms are described by classical statistics have been discussed.

DOI: 10.1134/S0021364018220137

1. INTRODUCTION

The study of physical systems allowing the controlled governing and exchange of microscopic states between light and a material carrier is very necessary for the development of quantum information technologies. The importance of solving the problem of a quantum interface has long been realized, as seen in reviews [1–5], but progress in this field is not too impressive. Theoretical estimates indicate that atomic ensembles are promising for experimental developments. There are certain achievements in both experimental observation and theoretical description of cooperative and coherent processes in such ensembles [6]. In quantum informatics, atomic systems are promising for the creation of quantum repeaters [2, 3] and for the development of quantum memory elements to create a single-photon source on demand [4, 5], which is a necessary element of a quantum optical processor. To successfully create a quantum interface for the case of interaction of optical radiation with systems of cold atoms, it is necessary, first, to overcome a fundamental difficulty associated with the quantum electrodynamic interaction of single atoms with a single photon and, second, to reduce the negative effect of diffraction divergence of a light pulse focused on an atomic system scale, which also reduces the efficiency of the interaction.

In the last decade, new experimental capabilities associated with the development of methods for the

optical control of quantum states of systems of ultracold atoms under their quantum degeneracy conditions have been revealed. Such systems are no longer unique laboratory objects. For example, the authors of [7] describe an experiment where an ensemble of ⁸⁷Rb atoms was cooled to a temperature of about tens of picokelvin. Optical monitoring methods are successfully developed to study processes of preparation and evolution of an atomic ensemble in a Bose–Einstein condensate (BEC) state [8, 9]. The interaction of atoms in the BEC state with optical cavity modes is used to control the spatial configuration of atomic ensembles [10, 11]. Transitions between different types of quantum degeneracy caused by the Fermi–Dirac and Bose–Einstein statistics in two-dimensional systems of cold atoms were studied in a number of experiments [12]. Methods developed for the optical control of states of atoms under quantum degeneracy conditions have innovative applications in problems of metrology and atomic interferometry [13–16].

The interaction of optical radiation with atoms can be significantly enhanced by involving cooperative effects that are manifested in ensembles of systems of atomic scatterers and effectively increase the coupling constant. This is brightly demonstrated by the coherent enhancement of the scattering of light on ordered and periodic structures that is caused by the Bragg diffraction mechanism and was observed in a number of experiments [17–25]. It is important that such a mechanism of strong coherent scattering is observed

in a wide spectral range and for atomic systems in different physical states.

In this review, we demonstrate that specific Bragg scattering on spatial inhomogeneities generated by interference of the order parameter is possible in the case of quantum degeneracy and the transition of an atomic gas to the BEC state [17, 18]. Under laboratory conditions, it is convenient to prepare periodic structures (atomic lattices) based on arrays of neutral atoms formed by optical traps in free space [19–22] or near a dielectric nanowaveguide [23–25]. The matter density modulation is a common factor responsible for the cooperative nature of the interaction of light with such physically different states of matter and for the possibility of coherent enhancement of scattering in certain directions. In this review, we present both common properties and qualitative differences between the optical properties of ordered systems of scatterers in different physical states. In particular, interference of material waves, which is observed in experiments with the BEC, forms in the optical transparency region a unique dielectric medium with the properties of a photon crystal that cannot be reproduced by an ensemble of neutral atoms with a classical spatial distribution.

The process of scattering is described within the microscopic quantum theory of scattering in multi-particle systems described in [6, 26–28]. Such an approach makes it possible to correctly take into account internal interactions and interatomic spatial correlations, which are important for the consistent description of the cooperative dynamics of the coherent scattering and spontaneous decay in an atomic subsystem. In particular, a closed equation was derived for a polariton propagator of a single-particle optical excitation in the BEC, which describes important corrections for the matter density in the quasi-energy structure of a system caused by both quasistatic and radiative interactions [26, 28]. Cooperative manifestations in the scattering of light by atomic systems that are in the BEC state and are described in the ideal gas approximation were considered in [29, 30].

In Section 2, we describe the method of calculation. In Section 3, the calculations for the scattering of light by an atomic system in the quantum degeneracy state are compared to those for an atomic chain that is located near a dielectric nanowaveguide and is interpreted as an array of classically distributed point scatterers.

2. MICROSCOPIC DESCRIPTION OF THE SCATTERING OF A PHOTON BY AN ATOMIC ENSEMBLE

In this section, we briefly present the basic principles of a microscopic approach to the description of the scattering of a single photon by a multiatomic ensemble.

2.1. General Formalism of the Scattering Problem

The consistent quantum-mechanical description of the scattering of a single photon on an atomic system is based on the formalism of the T -matrix defined as

$$\hat{T}(E) = \hat{V} + \hat{V} \frac{1}{E - \hat{H}} \hat{V}. \quad (1)$$

Here, $\hat{H} = \hat{H}_0 + \hat{V}$ is the total Hamiltonian, where \hat{H}_0 is the unperturbed Hamiltonian of the atomic subsystem and field and \hat{V} is the interaction operator. Scattering described by the transformation of the initial state $|i\rangle$ to the final state $|f\rangle$ is characterized by the differential cross section. This cross section can be expressed in terms of the scattering amplitude, which is the corresponding T -matrix element depending on the initial energy:

$$d\sigma_{i \rightarrow f} = \frac{\mathcal{V}^2 \omega^2}{\hbar^2 c^4 (2\pi)^2} |T_{g'e'k';gek}(E_i + i0)|^2 d\Omega. \quad (2)$$

The initial state of the system $|i\rangle = |g; \mathbf{e}, \mathbf{k}\rangle$ includes the photon state characterized by the wave vector \mathbf{k} , frequency $\omega \equiv \omega_{\mathbf{k}} = ck$, and polarization vector \mathbf{e} and the state of the atomic subsystem $|g\rangle$. The structure of this state depends on physical conditions: atoms can be considered as objects classically distributed in space or can be in a quantum degeneracy state, which requires the inclusion of the physical identity of atoms. In the limiting case of total degeneracy, for a rarefied medium with weak internal interatomic interactions, the state $|g\rangle = |BEC\rangle^N$ is a collective state of N atoms in the form of the BEC, which is described within Bogoliubov theory [31]. This state is primarily considered in this subsection.

The final state $|f\rangle = |g'; \mathbf{e}', \mathbf{k}'\rangle$ is specified by a similar set of quantum numbers, but the atomic subsystem in the general case is described by the perturbed state of the condensate $|g'\rangle$ for inelastic channels and the solid angle Ω is related to the direction of the wave vector of the scattered photon \mathbf{k}' with the polarization \mathbf{e}' . The quantization volume \mathcal{V} appears in the expression for the cross section because of the structure of interaction operators specified in the secondary quantization representation. In view of the unitarity of the scattering matrix, according to the optical theorem, the total scattering cross section can be expressed in terms of only one diagonal T -matrix element:

$$\sigma_{\text{tot}} = -\frac{2\mathcal{V}}{\hbar c} \text{Im} T_{ii}(E_i + i0). \quad (3)$$

The optical theorem is convenient for the calculation of the total scattering cross section in complex systems.

The interaction operator \hat{V} in Eq. (1) is defined in the dipole approximation and can be written in the secondary quantization representation

$$\hat{V} = -\sum_n \int d^3r \left[d_{nm}^\mu \hat{E}_\mu(\mathbf{r}) \hat{\Psi}_n^\dagger(\mathbf{r}) \hat{\Psi}_m(\mathbf{r}) + \text{H.c.} \right]. \quad (4)$$

Here, d_{nm}^μ is the matrix element of the μ th dipole moment component of the atom; the subscripts n and m specify the excited and ground states of the atom, respectively; $\hat{E}_\mu(\mathbf{r})$ is the μ th component of the electric field operator; covariant representation is used for vector and tensor quantities; and $\hat{\Psi}_m(\mathbf{r})$ and $\hat{\Psi}_n^\dagger(\mathbf{r})$ are the annihilation and creation operators of an atom at the point \mathbf{r} in the ground m and excited n internal states, respectively. The application of the dipole approximation in atomic systems with a density higher than one atom in the volume of the radiation wavelength faces certain difficulties (see [6, 32]). Our consideration is in essence limited by the model of weakly nonideal gas, where the internal interaction remains nevertheless significant and can be taken into account and described by the Gross–Pitaevskii equation (for details, see the remark in [28]).

We consider the BEC consisting of two-level atoms with the ground state 1S_0 and excited state 1P_1 , so that the quantum numbers $n = 0, \pm 1$ and $m = 0$ can be identified with the projection of the angular momentum of a single atom in the excited and ground states, respectively. For the ground state of the system existing in the condensate phase at zero temperature, we accept

$$\hat{\Psi}_0(\mathbf{r})|\text{BEC}\rangle^N = \Xi(\mathbf{r})|\text{BEC}\rangle^{N-1}, \quad (5)$$

where $\Xi(\mathbf{r})$ is the order parameter (the so-called “wavefunction”) of the condensate (see [33]). We consider the BEC as a macroscopic object so that the order parameter is insensitive to any small change in the number of particles in the condensate. Then, the scattering amplitude is given by the integral expansion

$$\begin{aligned} T_{fi}(E) &= \frac{2\pi\hbar(\omega'\omega)^{1/2}}{\mathcal{V}} \iint d^3r' d^3r \sum_{n',n} \\ &\times (\mathbf{d} \cdot \mathbf{e}')_{n'0}^* (\mathbf{d} \cdot \mathbf{e})_{0n} e^{-ik'\mathbf{r}' + i\mathbf{k}\mathbf{r}} \Xi^*(\mathbf{r}') \Xi(\mathbf{r}) \\ &\times \left(-\frac{i}{\hbar} \right) \int_0^\infty dt e^{\frac{i}{\hbar}(E - E_0^{N-1} + i0)t} iG_{n'n}(\mathbf{r}', t; \mathbf{r}, 0), \end{aligned} \quad (6)$$

where E_0^{N-1} is the energy of the initial state of the condensate consisting of $N - 1$ particles.

The scattering amplitude is determined by the Green’s function (propagator), which describes the propagation of a single optical excitation (polariton) in the condensate containing $N - 1$ particles

$$iG_{n'n}(\mathbf{r}', t'; \mathbf{r}, t) = \langle \text{BEC} | T \Psi_{n'}(\mathbf{r}'; t') \Psi_n^\dagger(\mathbf{r}, t) | \text{BEC} \rangle^{N-1}. \quad (7)$$

This function is the time-ordered production of Ψ -operators in the Heisenberg representation averaged over the condensate state and field vacuum:

$$|\text{BEC}\rangle^{N-1} \equiv |\text{BEC}\rangle_{\text{Atoms}}^{N-1} |0\rangle_{\text{Field}}. \quad (8)$$

The Ψ -operators are “dressed” because of interaction. It is assumed that the optical interaction is quasisonance so that the frequencies ω and ω' are close to the atomic transition frequency ω_0 .

Expression (6) for the scattering amplitude includes the order parameter, thus corresponding to the most methodically important case of the description of atoms as a degenerate quantum gas. In the opposite limit of the thermal ensemble with a temperature much higher than the critical value, atoms can be considered as scatterers located at certain spatial positions with the subsequent averaging over the thermal distribution (see [34, 35]). In this case, the order parameter and integration with respect to \mathbf{r} and \mathbf{r}' in Eq. (6) for the scattering amplitude should be replaced by sums over the atoms of the ensemble (see [6]).

2.2. Diagrammatic Expansion of the Green’s Function

The polariton propagator given by Eq. (7) can be constructed by the perturbation series expansion of Ψ -operators and the rearrangement of terms by means of the Feynman diagram technique (see [28, 35]). The result is the diagrammatic representation of the Dyson equation

$$\text{---} \text{---} \text{---} = \text{---} \text{---} \text{---} + \text{---} \text{---} \text{---} \text{---} \text{---} \text{---}, \quad (9)$$

where the double line with the arrow is the desired propagator, which is assumed to be dressed by all interaction processes, and the vertical arrows incoming to a vertex and outgoing from a vertex of the diagram are the order parameter and its complex conjugate, respectively. The corresponding block forms the self-energy part of the equation that physically describes the successive coherent conversion of excitation between the field and atom, which is accompanied by the recovery of the condensate state. This coherent process decays because of the possibility of spontaneous scattering and transition of the atom to the above-condensate state because of acquiring a certain recoil momentum.

The spontaneous decay mechanism is included in Eq. (9) through an incomplete polariton propagator, which is shown by the separated solid line and satisfies the Dyson equation separately including the contribution of spontaneous processes

$$\text{---} \text{---} \text{---} = \text{---} \text{---} \text{---} + \text{---} \text{---} \text{---} \text{---} \text{---}. \quad (10)$$

This equation should be considered together with the equation for the Green’s function for the time-ordered

vacuum average of the product of Heisenberg operators of the electric field



$$\text{wavy line} = \text{wavy line} + \text{wavy line with double-headed arrow} \quad (11)$$

These two diagrammatic equations constitute a closed system and should be solved together. This means that optical excitation produced in the condensate can result in spontaneous emission and this process is similar to incoherent scattering in the disordered gas with the same density. Indeed, Eq. (10) has a structure completely similar to the decay of the excited atom placed in a disordered medium of a weakly nonideal gas. Diagrammatic equation (11) formally determines the Green's function of the photon in such a dielectric medium [28, 33, 36] and the permittivity of the condensate.

2.3. Passage to a One-Dimensional Description

The solution of Eqs. (9)–(11) in three-dimensional geometry is a very difficult problem; the detailed description of the scheme and difficulties of the calculation can be found in [28]. The real calculation can be performed only for a one-dimensional system. Nevertheless, this calculation makes it possible to discuss a number of interesting physical effects caused by coherent scattering by periodic structures. We attribute this type of coherent scattering to the Bragg diffraction mechanism and to the modulation of the permittivity of matter (see Section 3.3).

Passage to a one-dimensional scattering problem implies the consideration of a layer of matter infinite in the transverse direction. We pass to the Fourier transform in the integrand considered now as a function of the energy and longitudinal coordinates z and z' . In view of the Dirac δ function of the transverse coordinates in the polariton propagator, the calculation of integral (6) over these transverse coordinates $dx dy$ and $dx' dy'$ gives the factor $\mathcal{L}_x \mathcal{L}_y$, which is partially compensated by a similar factor in the normalization volume $\mathcal{V} = \mathcal{L}_x \mathcal{L}_y \mathcal{L}_z$, and remains the normalization length $\mathcal{L}_z = \mathcal{L}$ in the one-dimensional problem.

As a result, the T -matrix element for the elastic forward and backward scattering has the form

$$T_{fi}(E) = \frac{2\pi\omega}{\mathcal{L}} \iint dz' dz \sum_{n,n'} (\mathbf{d} \cdot \mathbf{e})_{n'0}^* (\mathbf{d} \cdot \mathbf{e})_{0n} \times e^{-ik'z' + ikz} \Xi^*(z') \Xi(z) G_{n'n}(z', z; E - E_0^{N-1}), \quad (12)$$

where the frequency and polarization of the scattered photon are assumed to coincide with the respective parameters of the incident photon, i.e., $\omega' = \omega$ and $\mathbf{e}' = \mathbf{e}$; and we redefine $f \equiv i'$ to emphasize that the initial and final states for this type of scattering are equivalent.

It is convenient to pass from the T -matrix to the S -matrix, which relates the initial and final quantum states of the system (see [32, 37]), as

$$S_{fi} = \delta_{fi} - i \frac{\mathcal{L}}{\hbar c} T_{fi}(E_i + i0). \quad (13)$$

One-dimensional scattering is described by the transmission $\mathcal{T}(\omega)$, reflection $\mathcal{R}(\omega)$, and loss $\mathcal{L}(\omega)$ coefficients directly determined by the S -matrix as

$$\begin{aligned} \mathcal{T}(\omega) &= |S_{fi}|^2 \Big|_{k'=k>0}, \\ \mathcal{R}(\omega) &= |S_{fi}|^2 \Big|_{k'=-k<0}, \end{aligned} \quad (14)$$

$$\mathcal{L}(\omega) = 1 - \mathcal{T}(\omega) - \mathcal{R}(\omega),$$

which can be determined by solving Eqs. (9)–(11) in one-dimensional geometry.

3. BRAGG DIFFRACTION IN ONE-DIMENSIONAL STRUCTURES

In this section, we present the solutions of scattering equations for the case of periodic spatial structures. We consider different types of spatial modulation of the density of the medium, which can be due both to the modulation of the order parameter under quantum degeneracy conditions and directly to the ordered arrangement of atoms considered as point scatterers classically distributed in space. In the latter case, we address the scattering of light propagating in a mode of a one-dimensional dielectric waveguide with a subwavelength diameter by an ordered atomic chain located near its surface. Strong Bragg scattering in such a system was observed in experiments [24, 25] and the microscopic theory of this scattering was presented in [27]. We focus on the comparative analysis of scattering for these two physical examples in order to reveal both common properties and important differences associated with the fundamental difference of the classical and quantum descriptions of the spatial state of atoms.

3.1. Scattering of Light by the BEC

The fragmentation of the Bose–Einstein condensate accompanied by the strong coherent scattering of light by appearing spatial inhomogeneities of the order parameter was observed in a number of experiments [17, 18]. Within the one-dimensional model, we consider the fragmentation of the condensate as a result of the interference of two counterpropagating objects of the BEC in their center-of-mass system:

$$\begin{aligned} \Xi(z) &= \sqrt{2n_0} \cos\left(\frac{\pi z}{2L}\right) \cos(\Delta q z) \\ &= \sqrt{\frac{n_0}{2}} \cos\left(\frac{\pi z}{2L}\right) e^{i\Delta q z} + \sqrt{\frac{n_0}{2}} \cos\left(\frac{\pi z}{2L}\right) e^{-i\Delta q z} \\ &\equiv \Xi_+(z) + \Xi_-(z). \end{aligned} \quad (15)$$

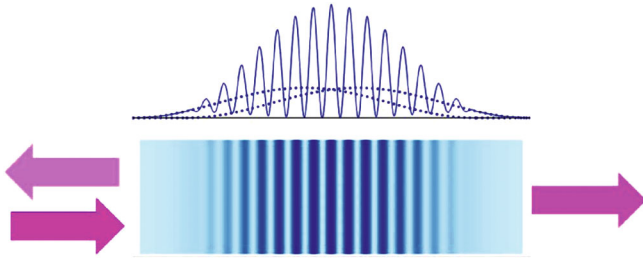


Fig. 1. (Color online) Geometry of the scattering of light on two fragments of the BEC that propagate with respect to each other and demonstrate the effect of nonlinear interference of material waves.

Here, the material wave is described by the order parameter $\Xi(z)$, and the interference of two wave fragments $\Xi_+(z)$ and $\Xi_-(z)$ forming it is responsible for the appearance of strong oscillations of the density with a spatial step of $\sim 1/\Delta q$ in their overlapping region characterized by the macroscopic scale L . The spatial density configuration $|\Xi(z)|^2$ thus appearing is illustrated in Fig. 1. This spatial density profile observed in the experiment [38] is an approximate solution of the Gross–Pitaevskii equation, is an example of nonlinear interference, and implies the motion of fragments at a quite high relative velocity.

The scattering of light in the regime of interference of material waves is very sensitive to the phase difference between complex functions $\Xi_+(z)$ and $\Xi_-(z)$, which is determined by the relative momentum of the condensate fragments (per atom) $2\hbar\Delta q$. The velocity of motion of fragments determines the scale of spatial oscillations of the BEC, which can be comparable with the wavelength of scattered radiation λ . As a result, the macroscopic BEC sample whose order parameter is modulated with a step comparable with the optical wavelength $2\pi/\Delta q \sim \lambda \ll L$ can be considered as a spatial lattice whose density has spatial modulation $\pi/\Delta q \sim \lambda/2$. The scattering (reflection within the one-dimensional model) of light through Wulff–Bragg’s diffraction mechanism will be observed in such a sample. The strong reflection of light from the formed diffraction lattice of the sample is illustrated in Fig. 2.

Figure 2 shows the transmittance \mathcal{T} and reflectance \mathcal{R} of a single photon as functions of its frequency detuning $\Delta = \omega - \omega_0$ from the resonant frequency of the atomic transition $\omega_0 = ck_0 = 2\pi c/\lambda_0$ presented in units of the spontaneous atomic decay rate γ .¹ These

¹ Strictly speaking, as shown in [28], because of the internal interaction, the transition frequency should be reduced by the chemical potential of the condensate μ_0 to $\tilde{\omega}_0 = \omega_0 - \mu_0/\hbar$ and the scattering spectrum should be redshifted. In view of the smallness of the chemical potential $\mu_0 \ll \hbar\gamma$, the corresponding correction is insignificant in the considered approximations.

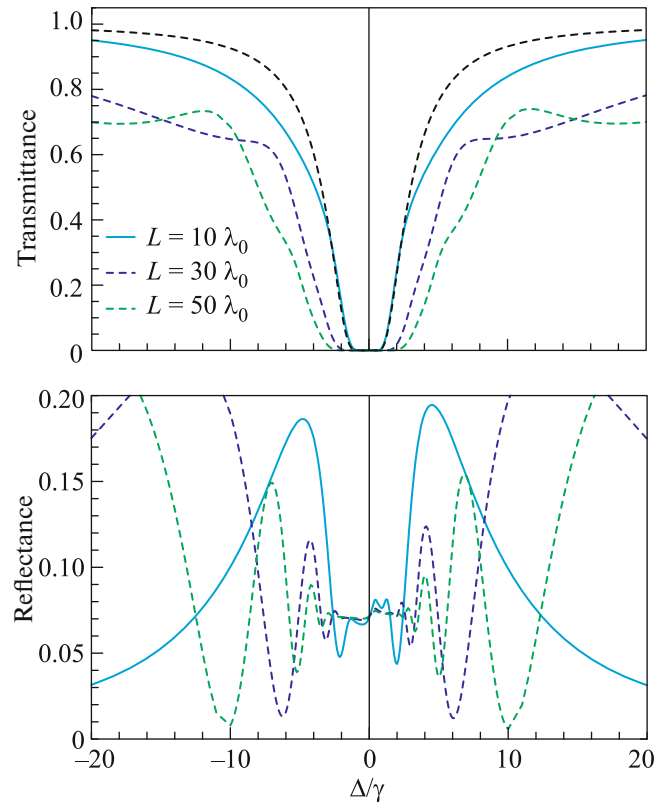


Fig. 2. (Color online) (Upper panel) Transmittance and (lower panel) reflectance versus the detuning of probe radiation $\Delta = \omega - \omega_0$ for an inhomogeneous atomic density distribution in the BEC specified by the order parameter given by Eq. (15) with $\Delta q = k_0 = \omega_0/c$, where ω_0 is the resonant frequency of the atomic transition for the geometry shown in Fig. 1. The dashed lines are reference dependences for the transmittance of light through an optically dense layer of a nondegenerate gas with the same density as the considered condensate. (Reprinted from [28] with permission of the American Physical Society.)

spectral dependences are presented for the longitudinal dimensions $L = 10\lambda_0$, $30\lambda_0$, and $50\lambda_0$, when the momentum of each of the condensate fragments per atom is $\hbar\Delta q = \hbar k_0 = 2\pi\hbar/\lambda_0$. Under these conditions, the distance between neighboring maxima in the density modulation $|\Xi(z)|^2$ is half the wavelength $\lambda_0/2$, which is optimal for the coherent enhancement of reflected light.

The spectral profile of the reflectance shown in the lower panel of Fig. 2 exhibits a very nontrivial behavior in different spectral ranges. Two main spectral ranges are seen. The first range is the resonance reflection region, where all considered samples reflect light almost identically. The second range is the asymptotic region far from the atomic resonance, where the detuning dependence of reflected light is strongly oscillating, oscillations are enhanced, and the spectral reflection range expands at the elongation of the sam-

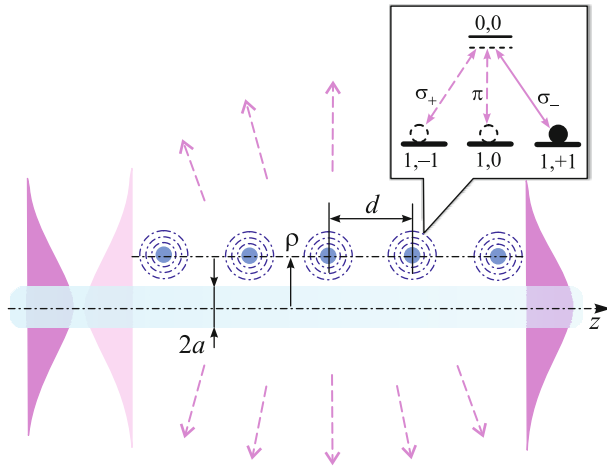


Fig. 3. (Color online) Geometry of the scattering of light propagating along a dielectric waveguide with a subwavelength diameter by an atomic chain with the period $d \sim \lambda^{\text{wg}}/2$. The atoms are located at the distance $\rho - a$ from the waveguide surface and their spins are oriented in the direction of light propagation. The optical transition σ_- in the atomic energy structure interacts predominantly with the fundamental mode HE_{11} of the waveguide in the left polarization. (Reprinted from [27] with permission of the American Physical Society.)

ple. It is very unusual for the spectral dependence of the reflectance that the scattering intensity increases far from resonance, where the weakening of the interaction of light with matter should seemingly be expected.

3.2. Scattering of Light by an Atomic Chain

As another example for comparison, we consider a system shown in Fig. 3, implying the one-dimensional scattering of light by atoms considered as point scatterers with a classical spatial distribution. Light propagates along a dielectric waveguide whose diameter $2a$ is comparable with the radiation wavelength and the external field is scattered by a chain of atoms that are located along the waveguide, are spaced by the distance $\rho \sim a$, and have the internal orientation of the spin moment in the direction of radiation propagation. The optical atomic transition σ_- approximately (in the paraxial approximation) corresponds to the waveguide mode in which radiation propagates. Atoms are ordered along the waveguide with the period $d \sim \lambda^{\text{wg}}/2$, where λ^{wg} is the wavelength of the waveguide mode differing from the vacuum value for the same frequency of light. The chosen $F_0 = 1 \rightarrow F = 0$ transition involving a nondegenerate excited state corresponds to the configuration of levels existing in the hyperfine structure of ^{87}Rb . It allows a simplified description of the excited atomic state by the renormalization of the radiative decay constant (for details, see [27]).

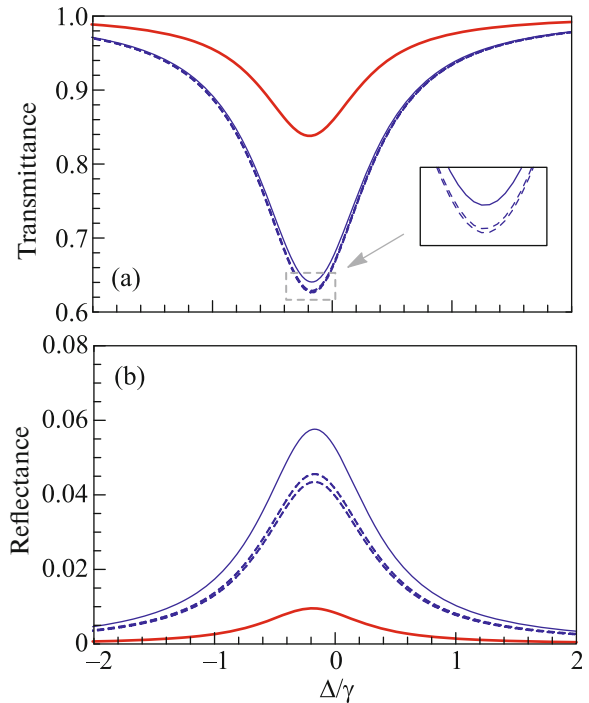


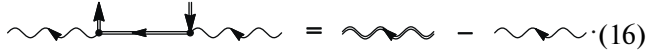
Fig. 4. (Color online) Spectral dependences of the (a) transmittance and (b) reflectance calculated for the scattering of light by a chain of five atoms separated by the distance $d = \lambda^{\text{wg}}/2$ and spaced from the waveguide surface at the distance $\rho - a =$ (thin blue lines) $0.5a$ and (thick red lines) a . For the case $\rho - a = 0.5a$, the partial contributions of the Rayleigh scattering channel with the conservation of (lower dashed lines) the polarization mode and (upper dashed lines) both polarization components. The solid line is the total contribution including Raman scattering channels (see Fig. 3). (Reprinted from [27] with permission of the American Physical Society.)

Figure 4 shows the calculated transmittance and reflectance of light through a chain of five atoms for two different distances $\rho - a$ from the waveguide surface and for different Rayleigh and Raman scattering channels. A noticeable reflection of light in the backward direction is observed because of the constructive interference of waves scattered by individual atoms. Such an interpretation based on Wulff–Bragg’s condition is only qualitative, implying a classical description of positions of atoms. The real calculation performed in [27] involves the microscopic evaluation of the resolvent of the Hamiltonian with the interaction operator given by Eq. (4) and the construction of the scattering T -matrix.

The scattering of light near atomic resonance is strong, exceeding scattering by a similar disordered structure. However, in contrast to scattering by a spatially modulated degenerate gas, the spectral dependences in this case are monotonic and the scattering intensity is concentrated in the spectral vicinity of atomic resonance and is much lower than that in the case of the BEC.

3.3. Comparison of the Results

What is the reason for such large differences in the spectra of radiation scattered by the BEC and atomic chain? To answer this question, we use the following diagrammatic relation between the polariton and photon propagators:



$$\text{Polariton propagator} = \text{Photon propagator} - \text{Polariton propagator} \quad (16)$$

First, this relation emphasizes that the atomic and field subsystems equivalently contribute to the formation of optical excitation in the condensate. Second, the diagram on the left side reproduces the structure of the scattering amplitude given by Eqs. (6) and (12). According to the Huygens–Fresnel principle [39], the right side of Eq. (16) describes the scattering of light in matter with the deviation of its propagation in free space.

Using the above relation, the solution of the one-dimensional scattering problem can be related to the solution of the one-dimensional wave equation

$$\frac{d^2}{dz^2} \mathcal{E} + \epsilon(z, \omega) \frac{\omega^2}{c^2} \mathcal{E} = 0, \quad (17)$$

where $\mathcal{E} = \mathcal{E}(z, \omega)$ is the positive-frequency complex component of the electric field propagating in the medium with the permittivity $\epsilon = \epsilon(z, \omega)$. This permittivity is a strongly oscillating function of the z coordinate. In the resonance case, the quantum spatial modulation of the order parameter and the corresponding modulation of the absorption coefficient are qualitatively simulated by a periodic structure of the atomic chain and both processes can be naturally attributed to diffraction under Wulff–Bragg’s condition.

However, the picture is significantly different at large detunings from resonance. In this case, the function $\epsilon = \epsilon(z, \omega)$ becomes real and close to unity but includes small rapidly oscillating correction to the average vacuum value. For an extended medium, this leads to the manifestation of properties of the photonic crystal and to the formation of the band structure near the atomic resonance frequency. At relatively small detunings, but under the condition $\Delta \gg \gamma$, a periodic dispersion dependence of the frequency on the wave-number appears in the wing of resonance. As a result, the incident wave excites two modes propagating in the opposite directions. Such a picture exists in a wide spectral range and, in view of the finiteness of the sample, leads to a complex oscillatory dependence of the reflectance and transmittance, which is observed in the lower panel of Fig. 2. Since the sample considered in the numerical calculation is finite, it is impossible to follow the structure of bands and the formation of the band gap, which should be observed at large detunings $\Delta \sim (n_0(\lambda/2\pi)^3)^{1/2} \sqrt{\gamma\omega_0}$.

Such a picture of the reflection of light cannot be reproduced by the configuration of atoms considered

as classically distributed scatterers (see Fig. 3). It would be required to prepare an atomic chain with a much higher linear density and the effective dielectric constant would be significantly larger than unity, which is typical of photonic crystals in semiconductor systems (see [40]). We also emphasize that the density modulation in the condensate is due to a deeply quantum effect of nonlinear interference between material waves and the internal motion of condensate layers.

4. CONCLUSIONS

The diffraction of electromagnetic waves scattered on periodic atomic structures has been known for more than a century. This phenomenon, later called Bragg diffraction, was studied at the beginning of the 20th century by several research groups, in particular, German physicist Max Theodor Felix von Laue, British physicists William Henry Bragg and William Lawrence Bragg, and Russian physicist George V. Wulff. The experiments clearly showed the periodic structure of solids and the wave nature of X rays. In this review, we have demonstrated that new experimental possibilities appearing at extremely low temperatures make it possible to observe new, very extraordinary, manifestations of Bragg diffraction caused by the wave behavior of atomic scatterers themselves.

The interaction of light with the Bose–Einstein condensate results in the formation of polariton excitation propagating along the sample and is consistently described by quantum scattering equations, where the atomic system is characterized by the wavefunction (order parameter) of the condensate. Although scattering can generally be interpreted within Maxwell’s macroscopic theory, the dielectric properties of the medium associated with quantum degeneracy and spatial modulation of the order parameter are unique and do not have any classical analog. In particular, a channel of strong coherent scattering of interfering fragments of the BEC appears even at a low density of the sample at large detunings in wings of atomic resonance in the spectral ranges where a normal gas with the same density would be transparent.

The coherent scattering mechanism discussed in this review can be interesting, e.g., for the development of effective quantum interface systems to minimize the number of atoms involved in the exchange of microscopic quantum states between light and matter. In current systems of optical cooling of atoms, it seems quite possible to localize a few atomic clusters in a compact trap by means of the optical tweezer method. As a result, a natural configuration appears where the scattering of light can be significantly enhanced by quantum density oscillations formed by the interference of material waves of localized atoms.

We are grateful to M.D. Havey for stimulating discussion of problems considered in this review. This

work was supported by the Russian Foundation for Basic Research (project no. 18-02-00265), by the Russian Science Foundation (project no. 18-72-10039), and by the Foundation for the Advancement of Theoretical Physics and Mathematics BASIS (project no. 18-1-1-48-1).

REFERENCES

1. E. S. Polzik, A. S. Sorensen, and K. Hammerer, *Rev. Mod. Phys.* **82**, 1041 (2010).
2. K. S. Choi, H. Deng, J. Laurat, and H. J. Kimble, *Nature (London, U.K.)* **452**, 67 (2008).
3. N. Sangouard, C. Simon, H. de Riedmatten, and N. Gisin, *Rev. Mod. Phys.* **83**, 33 (2011).
4. A. G. Radnaev, Y. O. Dudin, R. Zhao, H. H. Jen, S. D. Jenkins, A. Kuzmich, and T. A. B. Kennedy, *Nat. Phys.* **6**, 894 (2010).
5. X.-H. Bao, A. Reingruber, P. Dietrich, J. Rui, A. Dück, T. Strassel, L. Li, N.-L. Liu, B. Zhao, and J.-W. Pan, *Nat. Phys.* **8**, 517 (2012).
6. D. V. Kupriyanov, I. M. Sokolov, and M. D. Havey, *Phys. Rep.* **671**, 1 (2017).
7. T. Kovachy, J. M. Hogan, A. Sugarbaker, S. M. Dickerson, C. A. Donnelly, C. Overstreet, and M. A. Kasevich, *Phys. Rev. Lett.* **114**, 143004 (2015).
8. M. G. Bason, R. Heck, M. Napolitano, O. Eliaßon, R. Müller, A. Thorsen, W.-Zh. Zhang, J. J. Arlt, and J. F. Sherson, *J. Phys. B: At. Mol. Opt. Phys.* **51**, 175301 (2018).
9. D. J. Brown, A. V. H. McPhail, D. H. White, D. Baillie, S. K. Ruddell, and M. D. Hoogerland, *Phys. Rev. A* **98**, 013606 (2018).
10. D. S. Naik, G. Kuyumjian, D. Pandey, P. Bouyer, and A. Bertoldi, *Quantum Sci. Technol.* **3**, 045009 (2018).
11. V. D. Vaidya, Y. Guo, R. M. Kroeze, K. E. Ballantine, A. J. Kollár, J. Keeling, and B. L. Lev, *Phys. Rev. X* **8**, 011002 (2018).
12. A. V. Turlapov and M. Yu. Kagan, *J. Phys.: Condens. Matter* **29**, 383004 (2017).
13. T. Kovachy, P. Asenbaum, C. Overstreet, C. A. Donnelly, S. M. Dickerson, A. Sugarbaker, J. M. Hogan, and M. A. Kasevich, *Nature (London, U.K.)* **528**, 530 (2015).
14. S. Abend, M. Gebbe, M. Gersemann, H. Ahlers, H. Müntinga, E. Giese, N. Gaaloul, C. Schubert, C. Lämmerzahl, W. Ertmer, W. P. Schleich, and E. M. Rasel, *Phys. Rev. Lett.* **117**, 203003 (2016).
15. K. S. Hardman, P. J. Everitt, G. D. McDonald, P. Manju, P. B. Wigley, M. A. Sooriyabandara, C. C. N. Kuhn, J. E. Debs, J. D. Close, and N. P. Robins, *Phys. Rev. Lett.* **117**, 138501 (2016).
16. T. Laudat, V. Dugrain, T. Mazzone, M.-Z. Huang, C. L. Garrido Alzar, A. Sinatra, P. Rosenbusch, and J. Reichel, *New J. Phys.* **20**, 073018 (2018).
17. D. Schneble, Y. Torii, M. Boyd, E. W. Streed, D. E. Pritchard, and W. Ketterle, *Science (Washington, DC, U. S.)* **300**, 475 (2003).
18. A. Hilliard, F. Kaminski, R. le Targat, C. Olausson, E. S. Polzik, and J. H. Müller, *Phys. Rev. A* **78**, 051403(R) (2008).
19. B. J. Lester, N. Luick, A. M. Kaufman, C. M. Reynolds, and C. A. Regal, *Phys. Rev. Lett.* **115**, 073003 (2015).
20. D. Barredo, S. de Léséleuc, V. Lienhard, T. Lahaye, and A. Browaeys, *Science (Washington, DC, U. S.)* **354**, 1021 (2016).
21. M. Endres, H. Bernien, A. Keesling, H. Levine, E. R. Anschuetz, A. Krajenbrink, C. Senko, V. Vuletić, M. Greiner, and M. D. Lukin, *Science (Washington, DC, U. S.)* **354**, 1024 (2016).
22. E. Shahmoon, D. S. Wild, M. D. Lukin, and S. F. Yelin, *Phys. Rev. Lett.* **118**, 113601 (2017).
23. F. Le Kien, V. I. Balykin, and K. Hakuta, *Phys. Rev. A* **70**, 063403 (2004).
24. N. V. Corzo, B. Gouraud, A. Chandra, A. Goban, A. S. Sheremet, D. V. Kupriyanov, and J. Laurat, *Phys. Rev. Lett.* **117**, 133603 (2016).
25. H. L. Sorensen, J.-B. Béguin, K. W. Kluge, I. Iakoupov, A. S. Sorensen, J. H. Müller, E. S. Polzik, and J. Appel, *Phys. Rev. Lett.* **117**, 133604 (2016).
26. V. M. Ezhova, L. V. Gerasimov, and D. V. Kupriyanov, *J. Phys.: Conf. Ser.* **769**, 012045 (2016).
27. V. A. Pivovarov, A. S. Sheremet, L. V. Gerasimov, V. M. Porozova, N. V. Corzo, J. Laurat, and D. V. Kupriyanov, *Phys. Rev. A* **97**, 023827 (2018).
28. V. M. Porozova, L. V. Gerasimov, M. D. Havey, and D. V. Kupriyanov, *Phys. Rev. A* **97**, 053805 (2018).
29. M. G. Moore and P. Meystre, *Phys. Rev. Lett.* **83**, 5202 (1999).
30. Yu. A. Avetisyan and E. D. Trifonov, *Phys. Usp.* **58**, 286 (2015).
31. N. N. Bogolubov, *J. Phys. (USSR)* **11**, 23 (1947).
32. C. Cohen-Tannoudji, J. Dupont-Roc, and G. Grynberg, *Atom-Photon Interactions. Basic Processes and Applications* (Wiley, Weinheim, 1992).
33. E. M. Lifshits and L. P. Pitaevskii, *Course of Theoretical Physics, Vol. 9: Statistical Physics, Part II* (Nauka, Moscow, 1978; Pergamon, Oxford, 1980).
34. G. Placzek, *The Rayleigh and Raman Scattering* (Lawrence Radiation Laboratory, Berkeley, 1959).
35. V. B. Berestetskii, E. M. Lifshits, and L. P. Pitaevskii, *Course of Theoretical Physics, Vol. 4: Quantum Electrodynamics* (Nauka, Moscow, 1989; Pergamon, Oxford, 1981).
36. I. E. Dzyaloshinskii and L. P. Pitaevskii, *Sov. Phys. JETP* **9**, 1282 (1959).
37. M. L. Goldberger and K. M. Watson, *Collision Theory* (Wiley, New York, 1964).
38. M. R. Andrews, C. G. Townsend, H.-J. Miesner, D. S. Durfee, D. M. Kurn, and W. Ketterle, *Science (Washington, DC, U. S.)* **275**, 637 (1997).
39. M. Born and E. Wolf, *Principles of Optics: Electromagnetic Theory of Propagation, Interference and Diffraction of Light* (Pergamon, Oxford, 1959).
40. J. D. Joannopoulos, *Photonic Crystals: Molding the Flow of Light* (Princeton Univ. Press, Princeton, 2008).

Translated by R. Tyapaev